

## RESEARCH ARTICLE

### *Control of Movement*

# A paradigm to study the learning of muscle activity patterns outside of the natural repertoire

Ali Ghavampour,<sup>1,2</sup> Marco Emanuele,<sup>1,2</sup> Shuja R. Sayyid,<sup>2</sup> Jean-Jacques Orban de Xivry,<sup>3,4</sup>  
Jonathan A. Michaels,<sup>1,5</sup> J. Andrew Pruszynski,<sup>1,6</sup> and Jörn Diedrichsen<sup>1,2,7</sup>

<sup>1</sup>Western Center for Brain and Mind, Western University, London, Ontario, Canada; <sup>2</sup>Department of Computer Science, Western University, London, Ontario, Canada; <sup>3</sup>Department of Movement Sciences, KU Leuven, Leuven, Belgium; <sup>4</sup>Leuven Brain Institute, KU Leuven, Leuven, Belgium; <sup>5</sup>School of Kinesiology and Health Science, Faculty of Health, York University, Toronto, Ontario, Canada; <sup>6</sup>Department of Physiology and Pharmacology, Western University, London, Ontario, Canada; and <sup>7</sup>Department of Statistical and Actuarial Sciences, Western University, London, Ontario, Canada

## Abstract

The acquisition of novel muscle activity patterns is a key aspect of motor skill learning, which can be seen, for example, when beginner musicians learn new guitar or piano chords. To study this process, we introduce here a new paradigm that requires learning new patterns of flexion and extension of multiple fingers. First, participants practiced all the 242 possible combinations of isometric finger flexion and extension around the metacarpophalangeal joint (i.e., chords). We found that some chords were initially extremely challenging, but with practice, participants could eventually achieve them quickly and synchronously, showing that the initial difficulty did not reflect hard biomechanical constraints imposed by the interaction of tendons and ligaments. In a second experiment, we found that chord learning was largely chord-specific and did not generalize to untrained chords. Finally, we explored which factors made it difficult to produce some chords quickly and synchronously. Both variables were well predicted by the muscle activity pattern required by the chord. Specifically, chords that required muscle activity patterns that were smaller and more similar to muscle activity patterns required by everyday hand use could be produced more synchronously. Together, our results suggest that our new paradigm provides a valuable tool to study the neural processes underlying the acquisition of novel muscle activity patterns in the human motor system.

**NEW & NOTEWORTHY** In this study, we introduce a paradigm to study the learning of novel muscle activation patterns that deviate from those we are used to producing in everyday activities. Participants learned to produce different combinations of concurrent flexion and extension of 1–5 fingers of the right hand. We found that the ability to produce muscle activation patterns quickly and synchronously depended on how far they were from everyday hand activities.

*EMG; hand function; motor skill learning; muscle synergies; natural statistics*

## INTRODUCTION

The human motor system possesses a great capacity for learning new motor skills. Professional musicians and elite athletes vividly illustrate the range and complexity of movements that can be attained through repeated practice. Motor skill learning is a multifaceted process (1), involving a range of aspects from temporal sequencing of movements, fine control of speed and force, and more cognitive processes such as action selection and planning.

This paper focuses on a distinct aspect of motor skill learning: that is, the acquisition of novel muscle activity patterns. In fact, many tasks require the synchronous activation of specific combinations of muscles that are initially difficult to produce, possibly because they are not part of the existing motor repertoire. For example, the muscle activity pattern required to produce a certain guitar chord (e.g., F# chord) is initially challenging to achieve. Beginners often position their fingers one by one, deliberately using a sequential approach. After training, however, experts can produce the



Correspondence: J. Diedrichsen (jdiedric@uwo.ca).  
Submitted 20 February 2025 / Revised 31 March 2025 / Accepted 17 June 2025



same patterns quickly and synchronously. How novel muscle activity patterns are incorporated in the motor repertoire remains an open question, as well as which neuronal structures are involved in this process.

It is a common experience that some muscle activity patterns (e.g., grasping) are intuitive and easy, while others are difficult. One possible explanation is that muscle activity patterns that are needed for everyday hand movements span only a small subspace of all possible muscle combinations (2). This subspace may be represented by the nervous system as “muscle synergies.” According to this idea, muscle activity patterns that are far away from these “natural” synergies would be difficult to produce. Although there is considerable debate on the neural origin and function of muscle synergies (3–6), the idea that the human motor system has a strong tendency to activate muscles in a regular set of patterns is well supported (2). Here, we use the term muscle synergy purely at a descriptive level, referring to muscle activity patterns that the motor system can generate quickly and synchronously.

Following this definition, learning motor skills such as new guitar chords would require the acquisition of a novel muscle synergy. In the attempt to capture this learning process, we developed a well-controlled task, which required participants to produce muscle activity patterns that are outside of their natural repertoire. Our approach builds on prior work that examined finger combinations sampled from outside the typical movement subspace (7) and extends earlier paradigms that focused exclusively on flexion-only (8) or extension-only (9, 10) finger configurations around the metacarpophalangeal (MCP) joint. Here, we combined flexion and extension presses, resulting in 242 unique configurations (or “chords”), spanning a space from common to highly complex finger combinations.

In *experiment 1*, we verified that even though some chords were initially extremely hard to achieve, all could eventually be successfully mastered. In *experiment 2*, participants were trained on a limited set of four chords, showing that performance improvements reflect the specific acquisition of trained muscle activity patterns, rather than general learning. Finally, in *experiment 3*, we compared EMG recordings during chord production with those recorded during natural hand actions to show that the muscle activity patterns required for many chords lay well outside the distribution of patterns seen in natural hand use, and that the speed and finger synchrony for each chord related to its distance from this natural distribution.

## METHODS

### Participants

Fourteen healthy right-handed participants (mean age = 25.1 yr, SD = 2.5; 7 females) were recruited for *experiment 1*. For *experiment 2*, we recruited a different group of 14 healthy participants (mean age = 22.4 yr, SD = 3.1; 5 females), none of whom had previous experience with the task. Due to the potential influence of prior musical training (11), we did not recruit any professional musician. Participant had varying degrees of training with finger-based musical instruments (range 0–14 yr, mean = 4.4, SD = 5.4). Finally, 10 participants

among those who participated in *experiment 1* were also recruited for *experiment 3* (mean age = 25.9 yr, SD = 2.1; 5 females). All participants provided written informed consent before undergoing the experimental procedures. All procedures were approved by the Western University Research Ethics Board (ref 108479) and designed in accordance with the Declaration of Helsinki.

### Apparatus

Participants performed isometric finger presses in flexion/extension directions while keeping their right hand inside a custom-built device (12). The finger box was composed of two five-finger keyboards stacked on top of each other. Foam padding on each key ensured that fingers were comfortably restrained between the upper and lower keys. In addition, the finger box had an adjustable frame by which the space between the upper and lower keys could be adapted to accommodate different hand sizes. Force transducers (Honeywell, FS series, sampling rate = 500 Hz) above and below each key recorded the force exerted by each finger in extension/flexion direction (10 force transducers overall). Finger forces were mapped onto the vertical position of five cursors (white lines, Fig. 1B) projected on a screen, which moved up and down when the corresponding finger produced force in extension or flexion direction, respectively. The screen projection of the force produced by the ring finger and the pinkie was amplified by a factor of 1.5. This adjustment helped maintain the range of force required to produce chords feasible for all participants; participants were unaware of this adjustment. A gray rectangle marked the resting area (1.2 N flexion to 1.2 N extension; 0.8 N for ring and pinkie). Additional horizontal lines above and below the resting area indicated the flexion/extension response areas (2–5 N in both directions; 1.3–3.3 N for ring and pinkie; see Fig. 1). Across fingers and directions, the padding allowed for a ~1-mm upward and downward displacement of the finger.

### Task

At the beginning of each trial, participants had to keep the cursors inside the resting zone by maintaining their fingers relaxed. The trial began with a short 0.5 s announcement phase, where a chord was presented on the screen with a spatial visual cue (Fig. 1B: wait for go cue phase). A total of 242 of chords can be produced by combining finger flexion, extension, or holding still,  $242 = 3^5 - 1$  (all fingers still condition). Gray rectangles were presented inside the upper and lower response areas to prompt isometric flexion or extension of the corresponding finger. No rectangle indicated that the finger had to remain still. After 500 ms, the rectangles turned green, signaling the go cue. Participants were instructed to produce the required finger forces as quickly as possible. Successful chord production was achieved when the chord was held for 600 ms. If participants were unable to achieve the required chord within 10 s, the trial was marked as unsuccessful. Next, the rectangles disappeared, and participants were instructed to relax their fingers and return to the resting zone. After each trial, a number projected on the screen informed participants whether they successfully achieved the chord (1: successful trial, 0: unsuccessful trial). The following trial started after a 1-s intertrial interval. After

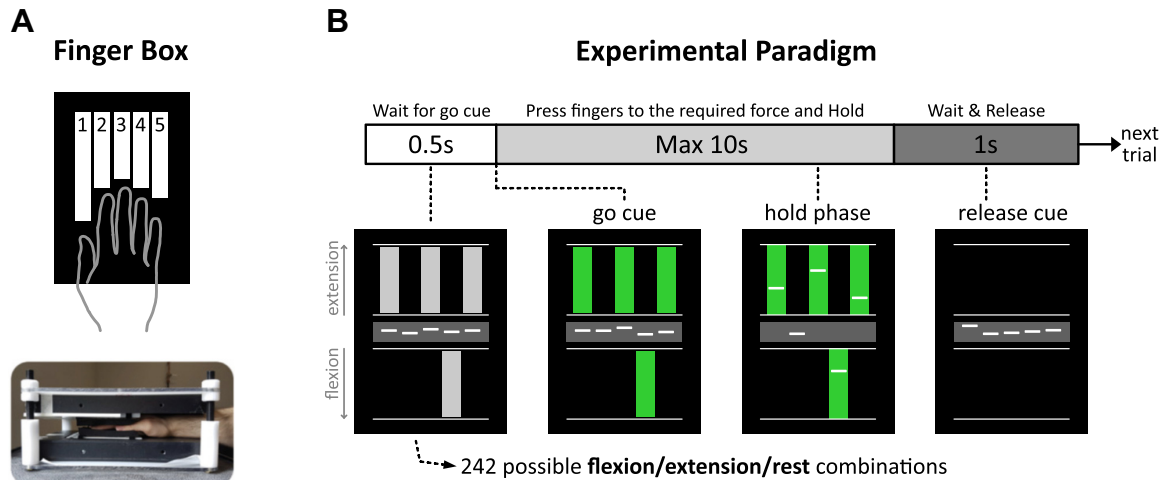


**Figure 1.** Synergy learning task. **A:** the finger box measured the isometric flexion and extension forces produced by the five fingers. **B:** the task. A spatial visual cue instructed the required forces for chords (here extension of D1, D3, D5, flexion of D4 and holding D2 still). The force level on each finger was indicated by white lines. After the cue turned green, participants had maximally 10 s to produce the required force pattern and hold it for 600 ms.

each block of trials, participants received feedback regarding their median execution time (time between the go-cue and the beginning of the 600-ms hold phase). To compensate for slight drifts in force transducers and the posture of the hand, each finger was calibrated by measuring the baseline force while participants were instructed to fully relax their fingers in the finger box.

## Experimental Procedures

**Experiment 1** aimed to characterize the speed and synchrony of every possible extension and flexion combination (i.e., chord). Participants practiced all 242 chords over 4 days, completing 1,210 trials per day, organized in 12 blocks (100 trials in the first 11 blocks, 110 trials in the last). Each day included five consecutive trials per chord. The order of chord presentation was fully randomized across days and participants. Participants were verbally instructed to produce the chords as quickly as possible and encouraged to reduce the execution time.

**Experiment 2** aimed to study the generalization in our paradigm by comparing improvements in trained chords with the generalization to untrained chords. We selected eight four-finger chords around the median of the mean deviation distribution (see *Performance Measures*) from days 3 and 4 of *experiment 1*. The selected chords were grouped into two sets of four chords. Participants practiced one of the two sets of chords (hereinafter “trained” chords) over five consecutive days, while the other set (“untrained” chords) was only tested on day 1 and day 5. Trained and untrained chord sets were randomly assigned, with seven participants training on set 1 and the other seven on set 2. The task and instructions were identical to *experiment 1*. Participants completed eight blocks of 50 trials each day. Each chord was repeated for five consecutive trials before moving to a different chord and the order of chord presentation was fully randomized across blocks and participants. On day 1 and day 5, trained and untrained chords were randomly intermixed in each block. The selected chords were group 1 [“EFEE-,” “EFF-E,” “E-EEE,” “FEF-E”] and group 2 [“FF-

EE,” “F-FEF,” “-EFEE,” “-FEFF”]. Letters E and F represent the Extension and Flexion of thumb to pinkie from left to right, while “-” means the finger must stay steady.

**Experiment 3** aimed to explore the factors that determine the speed and synchrony of chord production. It involved a single session in which we recorded the EMG from hand muscles (see *Electromyographic Recordings*) both during chord production and natural everyday hand actions. The chord task was structured as in *Experiments 1* and *2* and included 68 chords (10 one-finger, 30 three-finger, 28 five-finger chords). Three- and five-finger chords were selected from the lower, middle, and upper thirds of the mean deviation distribution from days 3 and 4 of *experiment 1*. This selection procedure ensured that we had chords of different levels of mean deviation for each number of fingers. We only selected a subset of the 68 chords to speed up data acquisition. Participants performed 680 trials (10 trials per chord), divided into 10 blocks, nine blocks with 70 trials, and the last block with 50 trials.

After completing the chord task, participants were moved to another experimental setup to record the muscle activity patterns occurring during natural hand actions. We designed a board containing a variety of everyday objects (Fig. 4C). This included natural activities such as grasping, rotating, pressing, sliding, drawing, writing, and manipulating objects of different shapes. Participants were asked to freely interact with any of the objects as they normally would. To further increase the diversity of the recorded natural hand actions, participants were also encouraged to interact with any object in the room beyond the board, including doors, cabinets, books in a bookshelf, light switches, an oscilloscope, a whiteboard and markers, a computer with mouse and keyboard. Although participants were encouraged to interact with a wide variety of objects, there were no specific instructions on the order and duration in which the objects were used. EMG was continuously recorded for ~20 min. Importantly, EMG electrode locations (see *Electromyographic Recordings*) remained identical between the chord and natural tasks to

ensure that the muscle activity patterns can be described within the same sensor space and are directly comparable.

## Performance Measures

Success rate of a chord was defined as the percentage of trials in which the chord was successfully achieved (and held for 600 ms) within 10 s after the go-cue.

Execution time was defined as the time interval between the go-cue and the beginning of the 600-ms hold phase. It therefore included both reaction time (RT; from go-cue to first force threshold crossing) and movement time (MT; from RT to the beginning of hold phase). Participants were given the goal to reduce their execution time, and they were provided with feedback about their median after each block of trials.

Mean deviation evaluates whether the chord was produced synchronously (i.e., as a single synergy), or whether it was produced as a sequence of finger presses. The force generated by the five fingers in each trial can be described as a five-dimensional trajectory,  $F \in \mathbb{R}^{T \times 5}$ , where  $T$  is the number of time samples between the moment the first finger left the resting zone until the correct force pattern was formed (500-Hz sampling frequency). If the fingers are pressed in perfect synchrony, the resulting trajectory will be a straight line ( $\vec{c}$ , dashed straight line in Fig. 2D) from  $\vec{0} \in \mathbb{R}^{1 \times 5}$  (resting force) to the final force pattern,  $\vec{f}_T \in \mathbb{R}^{1 \times 5}$ . If the chord was produced as a sequence of finger presses, the force trajectory would first go in the direction of the first finger, and then in the direction of the second (Fig. 2D, gray line), etc. As an overall measure of finger synchrony, we averaged the Euclidean distance of the produced force trajectory from the straight line across the chord execution (from the first force threshold crossing to the beginning of the hold phase).

$$\text{mean deviation} = \frac{1}{T} \sum_{t=1}^T \left\| \vec{f}_{t..} - \frac{\vec{f}_{t..} \cdot \vec{c}}{\vec{c} \cdot \vec{c}} \vec{c} \right\|_2$$

where  $\vec{f}_{t..}$  is the force of the five fingers at time sample  $t$ . Before the calculation, force traces were smoothed using a moving average window with a width of 30 samples (= 60 ms). Higher synchrony results in a mean deviation closer to 0. Importantly, mean deviation is independent of execution time, i.e., if participants produced the same sequence of finger presses more quickly, execution time would go down, but mean deviation would stay the same.

Response asynchrony was calculated for the chord-specific training study (*experiment 2*) where we had enough repetitions of a single chord. We introduced this measure to be able to express the asynchrony between fingers in terms of their relative timing. We defined the response time of each finger as the time when the derivative of the force crossed 20% of its peak in each trial. In this way, the response time is independent of the baseline force exerted by each finger. The overall response asynchrony between the fingers was then defined as the difference between the response time of the fastest and slowest finger in each trial.

## Electromyographic Recordings

### Electrode placement.

In *experiment 3*, we used a 10-channel surface EMG montage (Delsys, Trigno Research + System, Trigno Duo Sensors)

targeting the muscles acting on the metacarpophalangeal joints: the extensor digitorum communis (EDC), extensor digiti minimi (EDM) and extensor indicis (EI), extensors of the thumb (extensor pollicis brevis and longus), the flexor digitorum superficialis (FDS), abductor pollicis brevis (APB), and abductor digiti minimi (ADM) (Fig. 5A, top). Raw EMG signals were recorded at 2,148 Hz. Electrode locations were selected based on the anatomy of the target muscles and were optimized for each participant by asking them to perform isometric flexion/extension with individual fingers. The electrode was then placed on the surface location where muscle activity appeared maximal through palpation and EMG signal inspection.

### EMG preprocessing.

The signal from each EMG electrode (sampling rate 2,148 Hz, bandwidth 20–450 Hz) was demeaned, rectified, and low-pass filtered (6th order Butterworth filter, cut-off: 40 Hz). The same preprocessing was used for EMG recordings for both chords and natural hand actions.

### Chord muscle activity patterns.

We estimated the muscle activity patterns required for each chord by averaging the preprocessed EMG signals from each channel over the 600-ms holding phase and across trials. To account for gain differences across electrode sites, each channel was normalized by dividing by the Euclidean norm of activity across all chords.

### Distribution of natural muscle activity patterns.

After preprocessing, the EMG activity from natural hand actions was averaged within nonoverlapping 20-ms bins and normalized using the same channel-wise gain factor used for the chord EMG data. The binned normalized data were then partitioned into 10 sets. Each set contained bins sampled 200 ms apart by selecting every 10th bin. This approach reduced temporal dependence among samples, which is necessary for the kNN estimator (see *Pattern of muscle activity*).

## Models of Chord Speed and Synchrony

In the attempt to capture which factors influenced how quickly and synchronously a chord could be produced, we designed a set of linear models to predict the mean deviation and execution time of each chord using a range of characteristics. Because we wanted to test the predictive power of the muscle activity pattern, we restricted the modeling effort to the 68 chords studied in *experiment 3*. The dependent variable was the mean deviation (or execution time) from *days 3* and *4* in *experiment 1*, resulting in a 68-by-1 vector for each of the 14 participants. To cross-validate, each model was fitted to the data from 13 participants. The model's predictions were then correlated with the left-out participant, resulting in 14 correlation values. In the text, we report the predictive performance of models as the mean of these correlation values and the standard error of mean (SE) across participants ( $\bar{r} \pm \text{SE}$ ). Models were compared using paired  $t$  test.

### Noise ceiling.

Given that any performance measure is evaluated in the presence of measurement noise, no cross-validated model can reach a correlation of 1 with the data. To estimate the



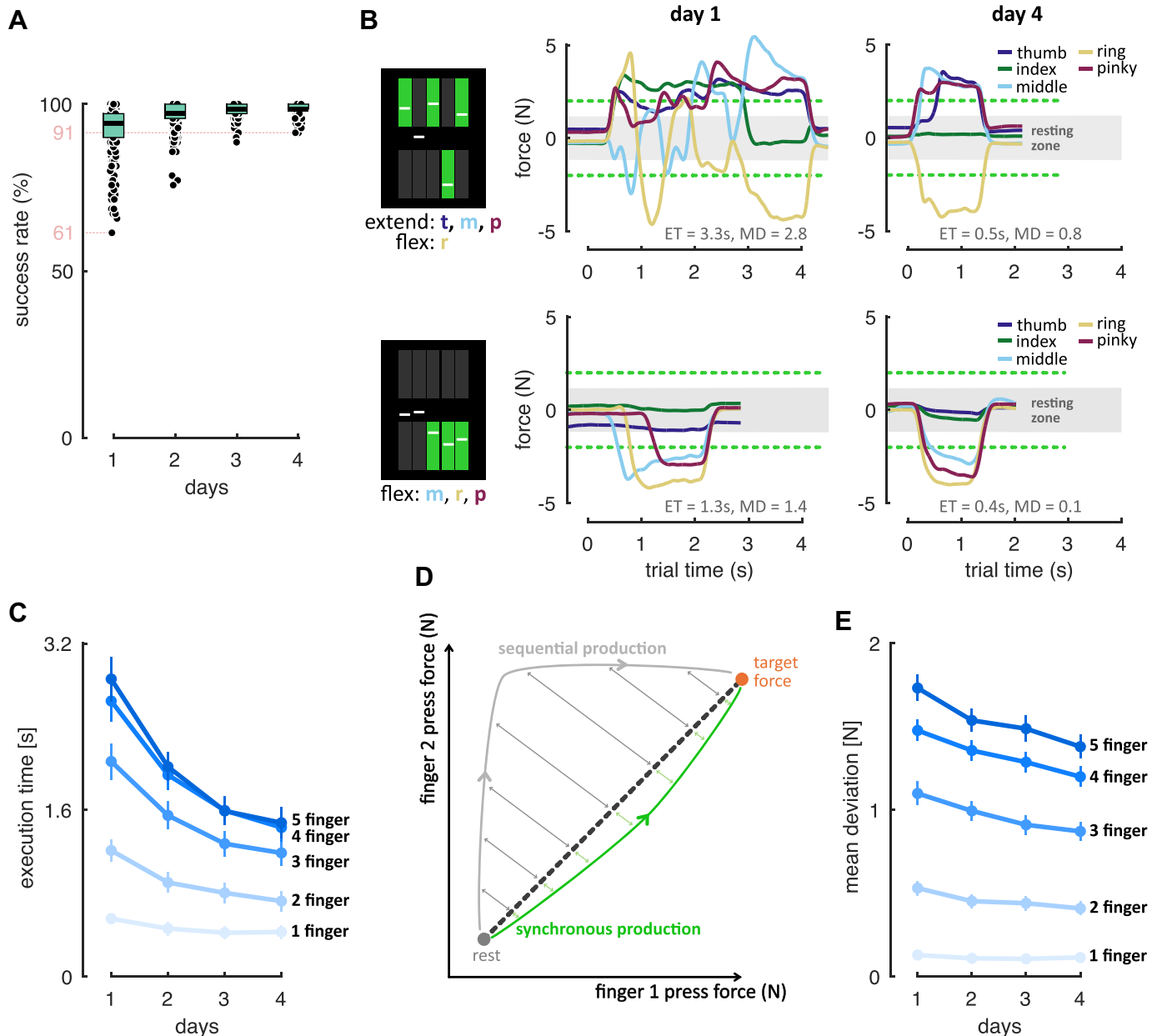


**Figure 2.** Experiment 1. **A:** success rate averaged across 14 participants within each day. Each dot represents a chord. Each box represents the median and interquartile range (IQR). **B:** example trials of two chords from two participants. The green dashed lines denote the minimal required forces in extension (top) and flexion (bottom) directions. Force from the ring and pinkie is scaled 1.5x for visual comparison with other fingers; 0 s is the go-cue. Execution time (ET) and mean deviation (MD) of the trials are labeled. **C:** average execution time (s) by day for different number of fingers. Error bars are SE across participants. **D:** schematic explanation of mean deviation. Perfect finger synchrony leads to a straight-line trajectory from rest to final force (dashed line). Examples of sequential (gray; high deviation) and synchronous (green; low deviation) force trajectories are plotted. Arrows denote the Euclidean distance from the straight-line. **E:** average mean deviation by day for chords with different number of fingers. Error bars are SE across participants.

noise ceiling, each participant's data were correlated with the group mean from which that participant was excluded. These 14 correlation values were then averaged to determine the noise ceiling for the models. The noise ceiling predicts the performance of a group model that captures all systematic differences across the group.

#### Baseline model.

Both mean deviation and execution time differed substantially for chords with different numbers of fingers (Fig. 2E). Increasing

the number of fingers will increase both the cognitive complexity of the stimulus and the motoric difficulty. Therefore, the number of fingers was included as baseline in all our models. We built a design matrix with columns corresponding to an indicator variable (0 or 1) for the number of fingers (three columns for 1-, 3-, and 5-finger chords of experiment 3).

#### Muscle activity pattern model.

The design matrix for this model corresponded to the average chord muscle activity patterns across participants (i.e., 68

chords by 10-EMG channels). The average success rate of participants in *experiment 3* was 99.57%, achieving almost 10 successful trials per chord and participant, giving a reliable EMG measurement.

### Force pattern model.

This model captured the amount and direction (flexion/extension) of the force generated by each of the five fingers. The design matrix for this model contained the force generated by each finger in extension and flexion direction averaged over the 600-ms holding phase across trials and participants (i.e., 68 chords by 10 forces, 5 regressors for flexion, 5 for extension).

### Visual complexity model.

This model aimed to capture the visual and perceptual complexity of the spatial cue used to instruct the chords (Fig. 1B). Visual complexity was quantified by counting how many times (in one chord) adjacent fingers received different instructions. For example, all five-finger flexion has zero transitions, while alternating flexion and extension of the five fingers results in four transitions. We built a 68 chords by five design matrix, with each column corresponding to an indicator variable (0 or 1) for the number of changes.

### Dissociating Muscle Activity Patterns to Magnitude and Pattern

#### Magnitude of muscle activity.

The magnitude of each chord's muscle activity pattern ( $\vec{m}_i \in \mathbb{R}^{10,1}$ ) was evaluated by calculating the Euclidean norm  $\|\vec{m}_i\|$ , which was then averaged across participants. This resulted in a 68-dimensional vector that was used as the group magnitude model.

#### Pattern of muscle activity.

We evaluated the probability of a chord's muscle activity pattern,  $\vec{m}_i \in \mathbb{R}^{10,1}$ , to belong to the distribution of natural muscle activity patterns, using an approach based on k-nearest neighbor density estimation. The goal was to estimate the probability of each chord's pattern belonging to the distribution of natural patterns regardless of the magnitude. Therefore, all muscle activity patterns (both chord and natural distribution) were normalized to unit length (see schematic in Fig. 6B). For each normalized chord muscle activity pattern ( $\vec{m}_i^*$ ), we then ranked the normalized muscle activity patterns from the natural distribution based on their Euclidean distance to  $\vec{m}_i^*$ . Let  $R_{k,i}$  denote the distance from  $\vec{m}_i^*$  to its  $k^{\text{th}}$  nearest neighbor in the natural distribution. The kNN density estimator estimates the density for  $\vec{m}_i$  by

$$\hat{p}_{\text{knn}}(i, k) = \frac{k}{n} \frac{1}{\text{volume of a } 10 - \text{dimensional ball with radius } R_{k,i}}$$

Due to the noisiness of the natural data, instead of choosing a single  $k$ , we found a more robust estimator for this density by integrating the results across  $k = 0.5$ . For this, we fitted a linear slope passing through 0 and the points defined by  $(\frac{1}{n}, R_{1,i}^{10}), \dots, (\frac{5}{n}, R_{5,i}^{10})$ . Because the distribution of probability estimates was strongly right skewed, we used the logarithm of this slope as a similarity measure of the chord pattern to the natural distribution. These log-probability

estimates (higher values indicated higher similarity) were closer to normal distribution.

To obtain a reliable estimate, the estimation was performed for each chord and each of the 10 natural distributions (see *Distribution of natural muscle activity patterns*) and then averaged across them. These estimates were then averaged across the 10 participants to derive a group similarity to natural statistics model.

### Alignment of Subspaces of the Muscle Activity Patterns for Chords and Natural Actions

To determine the relationship of the space of muscle activity patterns of the chords and the subspace of natural muscle activity patterns in a cross-validated fashion, we plotted the distribution of natural muscle activity patterns into two nonoverlapping splits: the first and third 5-min of data were concatenated to create the first split, and the second and fourth 5-min were concatenated to form the second split. Therefore, each split contained samples of different sets of actions. Principal component analysis within each split extracted 10 principal components (PCs). To cross-validate, the data from one split was projected to the PCs of the other split. The variance explained by PCs then reflects how aligned the probability distribution of natural muscle activities is between different sets of actions. Finally, we projected the 68 chord muscle activity patterns matrix onto the natural PCs to evaluate overall how the chords span the space of the muscle activity. Because natural and chord recordings were performed in the same session without changing electrode locations, the two datasets were directly comparable (see *Experiment 3*).

## RESULTS

### All Chords Were Biomechanically Possible

In *experiment 1*, participants were tasked to produce all 242 combination of finger flexion and extension (chords) each day for 4 days. We first wanted to establish whether each chord was biomechanically possible, and if yes, how quickly and synchronously participants were able to produce them. We therefore counted the number of trials in which participants could produce the chord (success rate). On *day 1*, the average success rate for some chords was as low as  $61 \pm 10.8\%$  SE across participants (Fig. 2A, *day 1*). This indicates that some chords were very challenging, as participants were unable to produce the required force pattern even with 10 s allotted per trial. Nonetheless, by *day 4*, even the most challenging chords were performed with nearly 100% success rate, with the least successful chord reaching a 91% (Fig. 2A, *day 4*). This indicates that no hard biomechanical limitations prevented chord production and that, with practice, participants could learn the muscle activity pattern required for each chord.

### Both Execution Time and Synchrony Improved with Practice

The main task goal for participants was to produce the instructed chord as fast as possible after the go-cue. As one performance measure, we therefore used execution time, the duration between the go-cue and the moment the correct force pattern was achieved. Execution time (Fig. 2C) showed

a significant main effect of day (repeated-measure ANOVA;  $F_{3,39} = 58.9$ ,  $P = 1.51\text{e-}14$ ) and number of fingers ( $F_{4,52} = 163.3$ ,  $P < 1\text{e-}16$ ), alongside a significant day  $\times$  number of fingers interaction ( $F_{12,156} = 41.2$ ,  $P < 1\text{e-}16$ ). Post hoc pairwise comparisons indicated significant improvement in execution time from *days 1* to *4* for all number of fingers (all  $t_{13} > 3.06$ , all  $P < 0.0046$ ). Therefore, chord production became quicker with learning from *day 1* to *4*. This improvement resulted from a reduction of both RT ( $t_{13} = 6.53$ ,  $P = 1.89\text{e-}5$ ) and MT ( $t_{13} = 7.10$ ,  $P = 8.05\text{e-}6$ ). Across chords, RT correlated positively with MT ( $r = 0.20 \pm 0.03$  SE).

Following our synergy definition, we hypothesized that if participants learned a new muscle synergy, they would not only produce the chord more quickly but also produce the chord as a single unit with all fingers pressing synchrony. Fast execution times could also be achieved by producing an asynchronous sequence more quickly. Therefore, we used mean deviation to measure synchrony between fingers independent of the speed of chord production. A schematic explanation of this measure is shown in Fig. 2D. For a sequential trial (gray trajectory; finger 2 is pressed before 1), the force trajectory (in 5-dimensional space) is far away from ideal synchronous trajectory (dashed line). For more synchronous production (green trajectory), the average distance from ideal synchronous trajectory is smaller. Because the distance is averaged across the entire execution time, this measure captures the relative asynchrony of the fingers, independent of the overall speed.

On *day 1*, many chords were produced with substantial time gaps between the fingers (see Fig. 2B), but performance gradually became more synchronous by *day 4*. Mean deviation (Fig. 2E) showed a significant main effect of day ( $F_{3,39} = 15.99$ ,  $P = 6.22\text{e-}7$ ) and number of fingers ( $F_{4,52} = 494.9$ ,  $P < 1\text{e-}16$ ), as well as a significant day  $\times$  number of fingers interaction ( $F_{12,156} = 9.53$ ,  $P = 1.03\text{e-}13$ ). Post hoc pairwise comparisons indicated significant improvement in mean deviation from *days 1* to *4* for 2- to 5-finger chords (all  $t_{13} > 3.96$ ,  $P < 0.00081$ ), but not significant for 1-finger chords ( $t_{13} = 0.91$ ,  $P = 0.19$ ). Furthermore, the trial-by-trial correlation of mean deviation and execution time was  $r = 0.653 (\pm 0.041$  SE), showing that fast execution was achieved by producing more synchronous finger presses.

### Learning is Chord-Specific

Our results from *experiment 1* indicate that chord production became quicker and more synchronous. Of course, this learning may not indicate the learning of specific, new muscle activity patterns, but rather reflect general improvements (e.g., through familiarization with the task and experimental equipment). In *experiment 2*, we therefore quantified how much of the performance improvement was specific to the practiced chords. We selected eight four-finger chords, which showed a medium mean deviation in *experiment 1*. From these, each participant was assigned four trained and four untrained chords (see METHODS). The trained chords were practiced for five consecutive days while untrained chords were only tested on *days 1* and *5*.

On *day 1*, execution time and mean deviation were not significantly different between trained and untrained chords (paired  $t$  test: both  $t_{13} < 0.57$ , both  $P > 0.58$ ; Fig. 3A). To assess chord specificity of learning, we measured the

difference between the last two blocks of the pretest to the first two blocks of the post-test (Fig. 3B). Both execution time ( $t_{13} = 6.14$ ,  $P = 3.52\text{e-}5$ ) and mean deviation ( $t_{13} = 5.48$ ,  $P = 1.05\text{e-}4$ ) of the trained chords improved significantly more than untrained chords (Fig. 3B). As in *experiment 1*, mean deviation and execution time were correlated on a trial-by-trial basis  $r = 0.650 (\pm 0.065$  SE), showing that improvements were not achieved through fast sequencing, but through synchronous force production.

For untrained chords, the change from pretest to post-test was not significant across participants in either measure (two-tailed one-sample: both  $t_{13} < 0.77$ ,  $P > 0.46$ ; Fig. 3B; red box). The general improvements were therefore very small compared with chord-specific improvements. This can also be seen in the example chord shown in Fig. 3C. In summary, we observed relatively little generalization of learning to the untrained chords.

### Quantification of Remaining Asynchrony after Practice

Although the reduction in mean deviation for the trained chords clearly indicated more synchronous performance, mean deviation did not approach 0 (i.e., perfect synchrony). Because mean deviation is a somewhat abstract measure, we also quantified the residual asynchrony between finger presses after learning by looking at absolute time difference between the response of the fastest and slowest finger in each trial (see METHODS). Mean absolute finger asynchrony on *day 5* was  $77.64 \pm 20.75$  ms (SE) for trained and  $121.13 \pm 32.37$  ms (SE) for untrained chords. This range of finger asynchronies suggests that the residual mean deviation may not reflect a deliberate sequencing of the motor commands delivered to the muscles but rather could reflect biomechanical interactions or motor noise.

### Minimal Changes in Force Patterns after Learning

Each chord required the production of a specific pattern of force directions, but we did not specify the exact force level for each finger. Thus, it is possible that participants not only got better at producing a specific force pattern but also changed the pattern of forces they produced. To test this, we averaged the finger forces during the hold phase across trials for each trained chord in *experiment 2*. We then performed eight repeated-measures ANOVAs (one for each chord) with day (*days 1* and *5*; 2 levels) and finger (5 levels) as within-subjects factors. Bonferroni correction was applied to control the family-wise error rate, resulting in a corrected significance threshold of  $P < 0.00625$ . The analysis revealed a significant main effect of day for one chord ("*E-EEE*",  $F_{1,6} = 170.30$ ,  $P = 9.98\text{e-}5$ ), but nonsignificant effects of day for the remaining seven chords (all  $F_{1,6} < 10.45$ , all  $P > 0.0178$ ). In addition, the day  $\times$  finger interaction was not significant for any chord (all  $P > 0.0123$ ). Thus, these results suggest that participants did not change the pattern of finger forces with learning in any systematic manner and only showed minimal reductions in the overall force.

### Factors Determining the Speed and Synchrony of Each Chord

To understand what needs to be learned for each chord to improve performance, it is useful to fully understand what

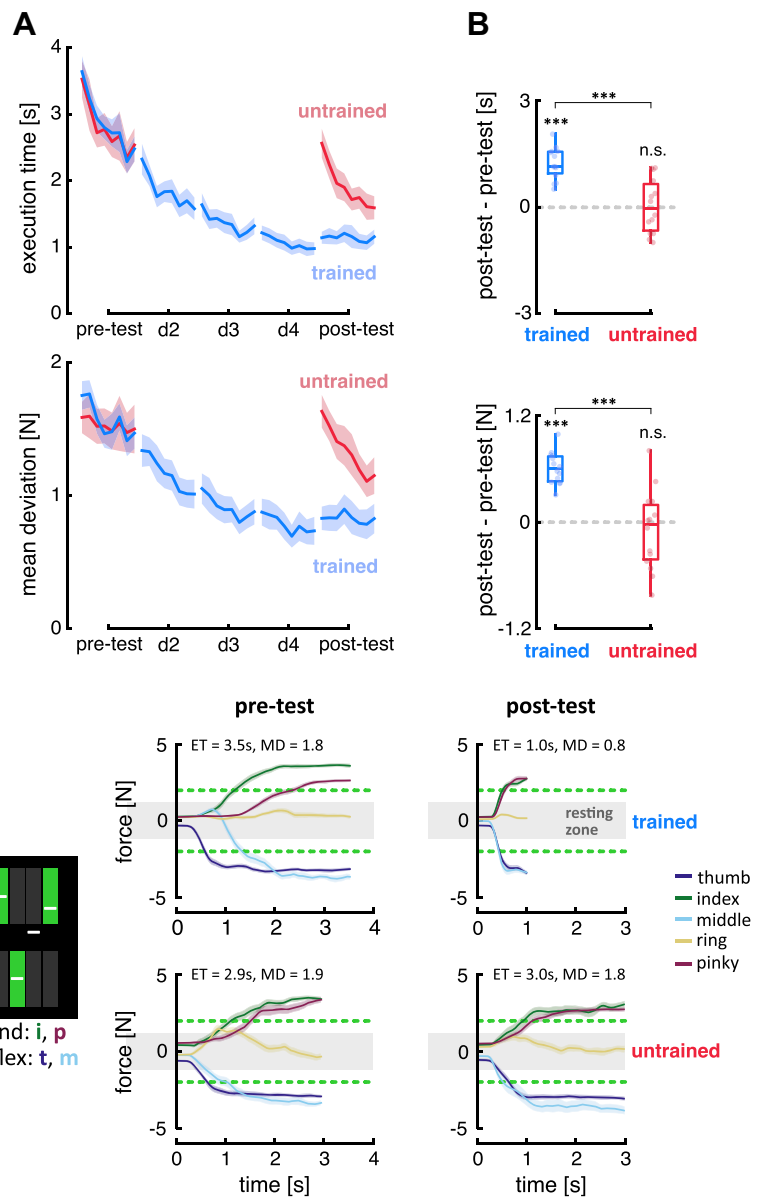


**Figure 3.** Experiment 2: chord-specific learning. **A:** average execution time and mean deviation for trained (blue) and untrained (red) chords by practice day. Lines represent the average performance across the eight blocks with shading representing the SE across participants. **B:** improvement of execution time (*top*) and mean deviation (*bottom*) for trained and untrained chords, as measured as the difference between the first two blocks of post test and the last two blocks of the pretest ( $***P < 0.001$ ). Box plots show the distribution of improvements across 14 participants. Each box represents the median and interquartile range (IQR). Each dot represents a participant. **C:** finger force traces averaged across all trials of pre- and post-test days. *Top* is when a participant trained on the chord and the *bottom* is for a participant for which the same chord was untrained. The shading represents the SE across the trials. Force traces are shown from go-cue to the average execution time ( $-ET$ ) labeled along with average mean deviation ( $-MD$ ). Force from the ring and pinkie is scaled  $1.5\times$  for visual comparison with other fingers.

makes certain chords harder in the first place. Being able to predict the baseline difficulty of each chord is also relevant for designing training studies in which we want to match sets of trained and untrained chords for initial performance. Here, we attempted to quantify the role of the visual complexity of the stimulus and motoric factors, such as the required force and muscle activity patterns, as determinants of difficulty. As a proxy for chord difficulty, we concentrated on mean deviation, as synchronous production was integral to our definition of a muscle synergy. As a secondary measure of difficulty, we also considered execution time. Note that mean deviation and execution time were highly correlated across the 242 chords ( $r = 0.82 \pm 0.05$  SE), suggesting that they are complementary measures of a common latent factor. To investigate the determining factors of chord synchrony, 68 candidate chords were selected based on *experiment 1*, including 1-, 3-, and 5-finger chords. The mean deviation measure of these chords, averaged across *days 3* and *4* of *experiment 1*, spanned a range between 0.045 and

1.870, indicating that they reflected the entire spectrum of chords that are very easy to very difficult.

### Noise ceiling.

Before building models to explain differences in difficulty, we established the noise ceiling, i.e., the maximal predictive performance we can expect from a group model (see *METHODS*). For this, we determined the average correlation of the mean deviation of the 68 chords from each participant with the group mean (with that subject left out). The average correlation was  $\bar{r} = 0.878 (\pm 0.0104$  SE) across the 14 participants of *experiment 1*. This high reliability means that the data permit the comparison of different group models.

### Baseline model.

In *experiment 1*, we found that chords involving more fingers had a significantly higher mean deviation. Many factors, including muscle activity and visual complexity, increase with the number of fingers. We therefore built a baseline



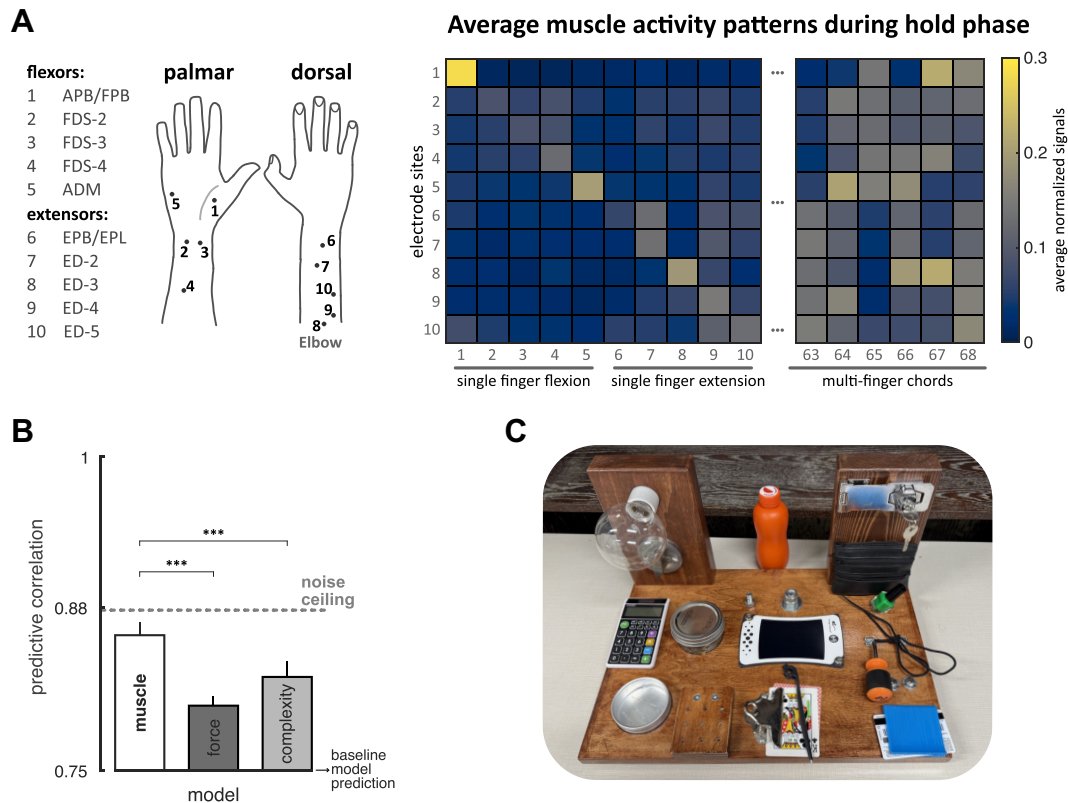


**Figure 4.** *Experiment 3.* **A, left:** dots indicate the approximate electrode locations on a participant's dorsal and palmar surfaces of the right hand. The intended muscles are labeled with numbers corresponding to these locations. **Right:** average EMG over the 600-ms hold phase, averaged across participants. **B:** cross-validated prediction performance (predictive correlation) of three models ( $***P < 0.001$ ). The lower limit is the prediction of the baseline model (number of fingers) and the upper limit (gray dashed line) is the noise ceiling. Error bars are SE across participants. **C:** a common object board used to assess the natural repertoire of hand muscle activity.

model (see METHODS) that predicts mean deviation as an arbitrary function of the number of fingers. This model achieved a predictive accuracy of  $\bar{r} = 0.750 (\pm 0.0083 \text{ SE})$ , indicating that a large portion of mean deviation can indeed be explained by this general factor. Nonetheless, the baseline model predicted the left-out data significantly worse than the noise-ceiling model ( $t_{13} = 10.89$ ,  $P = 3.33\text{e-}8$ ), which indicates that there were easier and harder chords within the groups of three- and five-finger chords, and that these differences were consistent across participants.

#### Muscle activity pattern.

This model predicted mean deviation as a linear function of the muscle activity pattern. To test this idea, in *experiment 3*, we recorded EMG from finger flexor and extensor muscles (Fig. 4A, left), while participants produced the 68 selected 1-, 3- and 5-finger chords. We averaged the rectified EMG during the hold phase (see METHODS) to estimate the muscle activity required for each of the 68 chords (Fig. 4A, right). We then predicted the mean deviation of chords (drawn from *experiment 1*) for each participant using a linear model of these 10 EMG channels (see METHODS). The model predicted the left-out mean deviation substantially better than the baseline model ( $\bar{r} = 0.8549 \pm 0.0102$ ,  $t_{13} = 9.37$ ,  $P = 1.89\text{e-}7$ , Fig. 4B). Although the performance was very close to the noise ceiling, it was still significantly lower ( $t_{13} = 10.31$ ,  $P = 1.26\text{e-}7$ ).

#### Force pattern.

Even though the muscle model predicted mean deviation well, the performance needs to be compared against other competing models. We considered that the difficulty may relate to the force direction produced by each finger. For example, chords involving the extension of the ring finger could be more difficult. This is especially the case, as we demanded the same force level for both flexion and extension and for different fingers, except for ring and pinkie, requiring 1.5 times less force. It is well known that different fingers have different maximum voluntary contraction force for flexion and extension (13). To capture these factors, we predicted the mean deviation from the average force pattern required by each chord (1 regressor per finger and direction; see METHODS). This model outperformed the baseline ( $\bar{r} = 0.8014 \pm 0.0077$ ,  $t_{13} = 9.95$ ,  $P = 1.90\text{e-}7$ ) but did not perform as well as the muscle model ( $t_{13} = 5.64$ ,  $P = 4.02\text{e-}5$ ; Fig. 4B), suggesting that muscle activity patterns carry more information about the difficulty than force direction.

#### Complexity of visual cue.

Alternatively, we considered that differences in performance between different chords may arise from the perceptual and cognitive processing of the visual cues that indicated each chord, independent of the amount of muscle activity and the force directions. Although we did not have an independent way of measuring visual “complexity,” any model based on

visual or cognitive factors would predict that two chords with same visual pattern (mirrored across the vertical or horizontal axis) should have the same complexity. To test this idea in a nonparametric way, we first grouped the chords with mirror-symmetric visual cues together, resulting in 69 groups among the 242 chords. From these 69 groups of equivalent visual complexity, 37 showed a significant difference ( $P < 0.05$ ) between chords in mean deviation. This number outstrips significantly the expected number of significant results under the Null hypothesis (5% of  $69 = 3.45$ ). This shows that the complexity of the visual cue alone is not sufficient to explain mean deviation.

To test how much variance of the mean deviation across chords this factor alone could predict, we designed a model by counting the number of transitions in the spatial visual cue of the chords (see METHODS). For example, all fingers flexion had zero complexity and alternating flexion, and extension of all fingers had four. Hence, this model is blind to the anatomical information from chords (i.e., which finger should press to which direction) and only captures the visual complexity of the chords. This model performed significantly better than the baseline model ( $\bar{r} = 0.8243 \pm 0.0124$ ,  $t_{13} = 6.51$ ,  $P = 9.84\text{e-}6$ , Fig. 4B). However, it performed worse than the muscle model alone ( $t_{13} = 5.004$ ,  $P = 1.21\text{e-}4$ ; Fig. 4B), again showing that perceptual or cognitive factors alone cannot fully account for chord synchrony.

### Dissociating Magnitude and Pattern of Muscle Activity

We then asked what characteristics of the chord muscle activity patterns determined how difficult a chord was to execute. A chord's muscle activity pattern is a point in the 10-dimensional space of muscle activations (Fig. 5A:  $\vec{m}_1, \vec{m}_2$ ).

The magnitude (or length) of the vector captures the overall activation of muscles required for a chord. In contrast, the direction of the vector is determined by the exact pattern of activity across muscles, independent of the magnitude. We explored which of these two factors predicted chord speed and synchrony better.

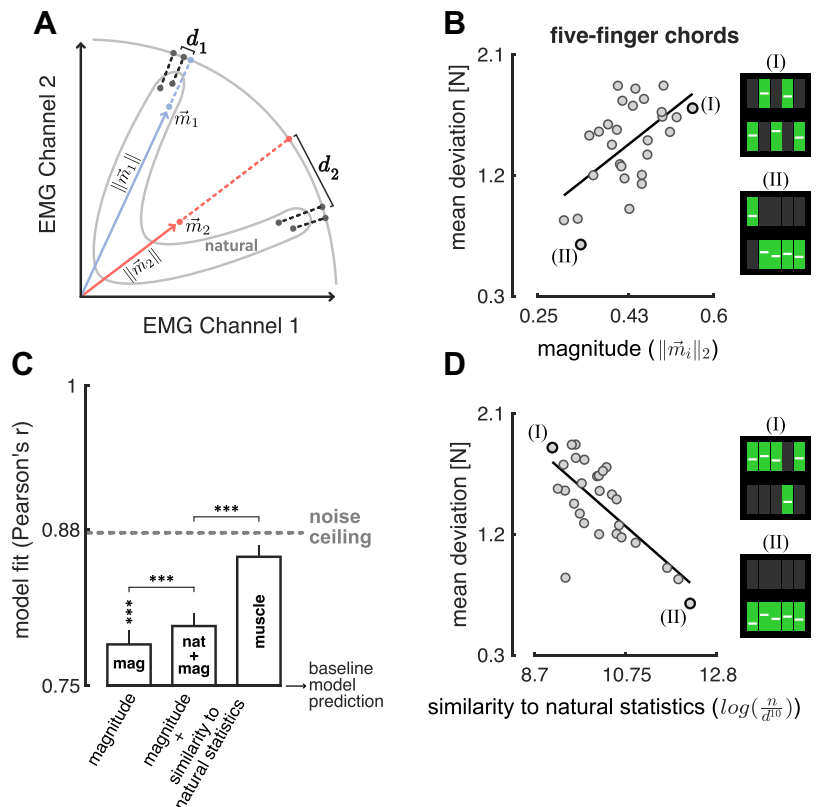
#### Magnitude.

Given that the overall force requirements were identical for all chords involving the same number of fingers, differences in the magnitude of muscle activity may indicate the need for co-contraction of muscles to compensate for the biomechanical interactions between fingers. We therefore predicted that chords that required a higher magnitude should be harder to produce synchronously. Indeed, the magnitude (Euclidean norm) of the chord muscle activity pattern correlated positively with mean deviation for 3-finger ( $\bar{r} = 0.418 \pm 0.035$ ;  $t_{13} = 11.901$ ,  $P = 1.15\text{e-}8$ ) and 5-finger chords ( $\bar{r} = 0.383 \pm 0.056$ ;  $t_{13} = 6.86$ ,  $P = 5.73\text{e-}6$ ; Fig. 5B), and positively but not significantly for 1-finger chords ( $\bar{r} = 0.092 \pm 0.077$ ;  $t_{13} = 1.19$ ,  $P = 0.119$ ). The magnitude model predicted the left-out data significantly better than the baseline model ( $\bar{r} = 0.787 \pm 0.012$ ;  $t_{13} = 4.32$ ,  $P = 4.17\text{e-}4$ ; Fig. 5C).

#### Pattern.

We also predicted that synchronous production should depend on the exact pattern of muscle activities. The motor system is likely to represent some muscle activity patterns common to natural actions as muscle synergies, such that they can be quickly and synchronously produced. We therefore predicted that if the pattern required by a chord is similar to these natural patterns, it would have lower mean

**Figure 5.** Magnitude and pattern explain the difficulty. **A:** schematic of evaluating the magnitude (Euclidean norm) and pattern (similarity to natural statistics models) factors.  $\vec{m}_i$ s represents two chord muscle activity patterns. The distribution of natural muscle activity patterns is plotted. **B:** average mean deviation versus average magnitude for five-finger chords. The chords at the two extremes of both estimates are labeled. **C:** prediction correlation of magnitude, natural + magnitude, and muscle activity pattern models ( $***P < 0.001$ ). The lower limit is the prediction of the baseline model (number of fingers) and the upper limit (gray dashed line) is the noise ceiling. Error bars are SE across participants. **D:** average mean deviation versus average similarity to natural statistics for five-finger chords.



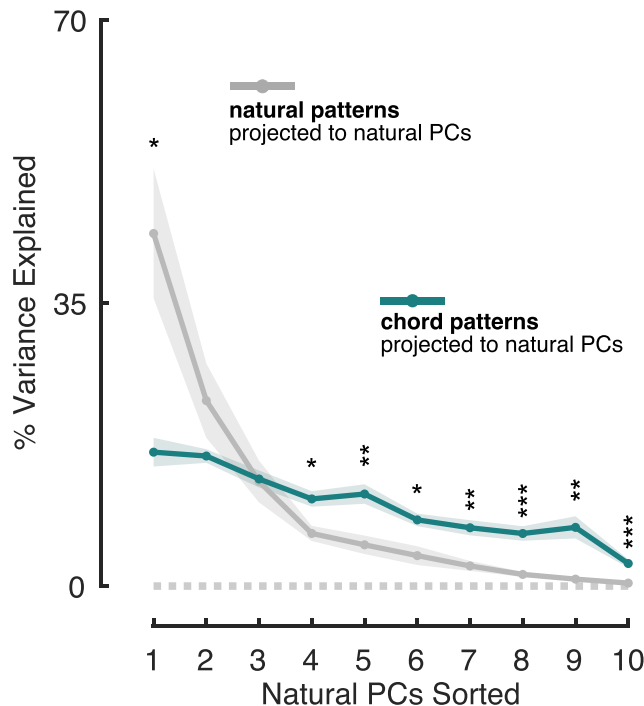


**Figure 6.** Variance of natural and chord muscle activity patterns projected on every natural PCs. The shading is SE across participants. PCs are sorted based on the variance they explain in natural patterns. Stars denote the significance of two-sample *t* test between the variances (\**P* < 0.05, \*\**P* < 0.01, \*\*\**P* < 0.001).

deviation. Within *experiment 3*, we therefore also collected EMG while the participants performed naturalistic hand activities, interacting with a number of common objects (Fig. 4C; see METHODS, *Experiment 3*). To determine whether the estimated distribution of natural muscle activity patterns depends on the specific actions that were performed, we split the data into the first and second 10 min of data recording. Participants interacted with different objects in a random order across these two halves. We calculated a cross-channel correlation matrix of EMG activities in each half of the data. The split-half correlation was  $r = 0.859 (\pm 0.037 \text{ SE})$ , indicating that the distribution of muscle activities was relatively independent of the specific actions performed (2, 14, 15) and could be measured in a reliable manner.

From the entire data, we then formed the nonparametric model of the distribution of natural muscle activity patterns (see METHODS). To only account for the pattern, the magnitude was normalized between natural and chord (Fig. 5A). Then, we estimated how likely a chord pattern would be under this natural distribution (see METHODS). These estimates correlated negatively with the mean deviation of 1-finger ( $\bar{r} = 0.223 \pm 0.068$ ;  $t_{13} = 3.27$ ,  $P = 3.02 \times 10^{-3}$ ), 3-finger ( $\bar{r} = 0.312 \pm 0.023$ ;  $t_{13} = 13.78$ ,  $P = 1.96 \times 10^{-9}$ ), and 5-finger chords ( $\bar{r} = 0.451 \pm 0.034$ ;  $t_{13} = 13.08$ ,  $P = 3.71 \times 10^{-9}$ ; Fig. 5D). The natural statistics model added on top of the magnitude model significantly outperformed the magnitude alone in predicting the left-out data ( $\bar{r} = 0.801 \pm 0.011$ ;  $t_{13} = 6.897$ ,  $P = 5.45 \times 10^{-6}$ ; Fig. 5C). This confirmed that, independent of the magnitude, the closeness to the natural distribution of muscle activity patterns can predict how synchronous a chord could be produced.

## Predicting Execution Time

In our main analysis, we concentrated on mean deviation of the chords as a measure of motoric difficulty. We obtained similar results using execution time. The noise ceiling of the execution time was lower than for mean deviation, at  $\bar{r} = 0.6815 (\pm 0.0237 \text{ SE})$ . Again, the muscle activity pattern model outperformed both force pattern and the complexity of the visual cue models in predicting execution time ( $\bar{r} = 0.6717 \pm 0.035$ ;  $t_{13} > 3.54$ ,  $P < 0.0018$ ). In contrast to mean deviation, the muscle activity pattern model reached the performance of noise ceiling ( $t_{13} = 1.44$ ,  $P = 0.17$ ). As before, the magnitude model significantly outperformed the baseline model ( $\bar{r} = 0.604 \pm 0.020$ ;  $t_{13} = 2.80$ ,  $P = 0.0075$ ) and the natural statistics model combined with the magnitude model significantly outperformed the magnitude model alone ( $\bar{r} = 0.619 \pm 0.017$ ;  $t_{13} = 2.65$ ,  $P = 0.01$ ).

## Chords Span the Space of Possible Muscle Activity Patterns

Finally, we designed our task such that the muscle activity patterns associated with the set of chords would exhaustively span the space of possible hand muscle activity patterns. It is well known that muscle activity pattern associated with natural hand movements mostly lie within a low-dimensional subspace (2). We therefore wanted to ensure that some of our chords required muscle activation patterns that fell outside of that space. To quantify this, we used principal component analysis to extract the 10 principal components (PCs) of the natural muscle activity patterns. Using cross-validation (see METHODS), we then determined what proportion of the variance was captured by these dimensions using muscle activity recorded during other manual actions. The results (Fig. 6) revealed the expected low-dimensional structure of the natural muscle activity patterns, such that PC 6 to 10 only accounted for 8.92% of the variance.

We then projected the chord patterns onto the natural PCs. This revealed a much flatter distribution of variance, where the five-dimensional subspace that was least visited by natural hand actions accounted for 31.95% of chord variance. This shows that a substantial portion of the muscle activity patterns for the chords required muscular patterns that were rarely produced during natural hand use.

## DISCUSSION

In this paper, we developed a new paradigm to study the acquisition of novel hand muscle activity patterns (“muscle synergies”) that are outside the current behavioral repertoire. Intuitively, this is an important aspect of many skill learning tasks, such as playing the guitar or piano. Our paradigm targets synergy learning by asking participants to perform “chords”—i.e., combinations of isometric finger flexion and extension at the metacarpophalangeal joint. In *experiment 1*, we included all the 242 possible chords that can be formed by flexing or extending any combination of 1–5 fingers independently. Some of these hand configurations could be performed immediately and almost effortlessly (e.g., isometric flexion of the index finger), others were much more challenging. On *day 1*, participants failed to produce the most challenging chords in nearly 40% of the trials. This

initial low success rate is remarkable, considering that we allowed a 10-s window to achieve chords and repeated each chord five times. The allowed time window largely exceeds the usual timescales of everyday voluntary movements and should be sufficient to achieve any force pattern within participants' motor repertoire. One possibility is that the biomechanical constraints imposed by the intricate interplay of muscles and tendons may prevent the execution of some chords (16). Tendons and ligaments show quite substantial intersubject variability (17–19); thus, it was not clear a priori that all individuals would be able to produce all chords. However, after 4 days of practice, all 14 participants achieved all chords with nearly 100% success rate. This suggests that all 242 hand configurations are biomechanically possible within the relatively low force range required by the paradigm. Therefore, the most challenging chords likely demand muscle activity patterns that the untrained motor system simply cannot produce. The successful production of these chords after practice therefore suggests the acquisition of new neural representations supporting their execution.

Chords can be achieved by two different strategies: one is to produce the isometric force of each finger sequentially until the desired configuration is reached. This strategy simplifies the problem of controlling different muscles synchronously. Once the required force for one finger is achieved and the corresponding muscle pattern stabilized, another finger is activated, gradually forming the full chord configuration. Indeed, some subjects chose this strategy in the initial part of their training. The improvement in mean deviation across training sessions, however, shows that participant did not improve their execution time solely by producing the same sequence faster. Instead, participants activated the relevant muscles more synchronously. This second “synergistic” strategy suggests that participants formed new chord representations, which allowed them to recruit the corresponding muscle activity pattern both rapidly and synchronously.

This conclusion is also supported by the results of *experiment 2*. Here, participants practiced only four four-finger chords. Their performance was assessed before and after training on these four trained chords, as well as on a separate set of untrained chords. Both execution time and mean deviation improved in a chord-specific fashion, with only marginal improvement on untrained chords. This suggests that chord learning mostly occurs through the formation of specific motor representations for the trained chords. Previous studies have reported some degree of generalization in similar tasks (8, 9). However, these effects were asymmetric: improvements in extension-only chords generalized to flexion-only chords, but not the reverse (9). In our experiment, the trained chords spanned a range of flexion and extension of different fingers (see METHODS), such that generalization in force or muscle space should have become visible in our paradigm. However, we observed only marginal improvements, suggesting that generalization was limited for the specific chords that participants trained on. The exact patterns of generalization between chords remains an interesting topic for future research.

Furthermore, it remains unclear where chord-specific learning occurred along the continuum of visual, cognitive, and motor processes required for chord execution. Our results do not allow a definite answer. However, some initial insights can be gleaned by assessing which factors make

some chords more difficult than others in the first place. Clearly, chords become more challenging as the number of involved fingers increases. However, the number of fingers alone does not fully capture the systematic differences in mean deviation across chords. To determine the most likely explanation for these differences, we compared a range of different models. The model based on the muscle activity patterns outperformed one based on visual complexity. The model also outperformed a model based on finger and force directions, which, for example, captures the fact that ring finger extension is more difficult to achieve than index finger flexion. This is especially important as we use the same low force level for extension and flexion, even though the maximum voluntary contraction (MVC) for finger flexion is approximately twice as large than for extension. Although the different difficulty of the constant force target across fingers and directions may certainly have contributed to our results, the relatively poor performance of the force model indicates that muscle activity pattern required to produce the chord was a more important factor for predicting difficulty. In summary, this suggests that some (if not all) of the chord difficulty is due to the lack of suitable muscle synergies, rather than due the cognitive or perceptual load of interpreting the complex visual cue or the amount of force that needs to be produced.

Mean deviation also scaled with both the magnitude of muscle activity and the similarity of chord muscle activity patterns with those occurring during everyday actions. The latter finding provides evidence that chord performance is indeed constrained by existing synergies. Chords requiring muscle activity patterns similar to those used in everyday motor tasks (e.g., precision/power grip) are easier to achieve compared with those absent in the natural hand repertoire. In other words, learning novel muscle activity patterns may require expanding the current repertoire of motor representations beyond the limited set of existing synergies.

In a related set of studies, participants were asked to acquire an arbitrary mapping between muscle activity or joint kinematics of the upper limb and the two-dimensional position of a visual cursor (20–24). To some degree, this paradigm(s) requires to learn novel muscle activity patterns. On the other hand, participants were free to choose any pattern in N-dimensional EMG or kinematic space that would map to the same two-dimensional cursor movement. With only two controlled dimensions, it is likely that they chose muscle activity patterns that were closer to their natural repertoire. A key advantage of our paradigm is that it encompasses independent flexion and extension across the five fingers, forcing participants to acquire specific muscle activity patterns, “non synergistic” ones.

The new paradigm introduced in this work is designed to be used in future research addressing the neural correlates of synergy learning with different techniques, including noninvasive brain stimulation and neuroimaging. In this regard, one important question is where new synergy representations are formed along the motor hierarchy—from action selection to execution. Previous work suggests that, in sequence learning, new skill representations are not purely motoric but operate at a more abstract level, controlling the sequence of individual movements rather than directly encoding the corresponding muscle activity patterns (25).



According to this view, sequence production may rely on the sequential recombination of existing muscle synergies. In support of this idea, a recent study showed that plastic changes accompanying sequence learning mostly occur in high-order motor cortical areas, while being almost absent in the primary sensorimotor cortex (26, 27). Chord learning may share similar principles. Novel muscle activity patterns may be achieved through high-level skill representations combining existing muscle synergies (7). Alternatively, chords may be achieved through the formation of new motor representations at lower hierarchical level, such as in M1 or spinal cord. We found that the produced force patterns during the hold phase remained largely unchanged after 5 days of practice. This feature of our design allows for the examination of neural and muscle activity pattern changes across learning without confounding effects from behavioral variability.

A second important question is how multifinger hand configurations are represented across motor cortical areas. Do multifinger representations reflect the linear combination of single-finger activity, or do they involve completely orthogonal representations? Current findings are inconclusive. Intracortical recordings performed in the human premotor cortex support the pseudolinear hypothesis (28). On the other hand, fMRI activity during single- and multifinger sensory stimulation suggests that the activity patterns for the individual fingers combine predominantly linear in area 3b but show a rich and nonlinear behavior in M1 (29). Our task now offers ample opportunity to address these problems in future studies by comparing fMRI activity for single- and multifinger chords after practice.

## DATA AVAILABILITY

The preprocessed data (performance measures, average hold force, average EMG, magnitude and natural statistics estimates, etc.) are available (<http://doi.org/10.6084/m9.figshare.29066687>). Raw data are available upon request from the first author.

## ACKNOWLEDGMENTS

We thank Thu Mai for help with data collection on *experiment 2*.

## GRANTS

This work was supported by a CIHR Project Grant to J.D. and J.A.P. (PJT-175010), a Canada Research Chair to J.A.P., and the Canada First Research Excellence Fund (BrainsCAN).

## DISCLOSURES

No conflicts of interest, financial or otherwise, are declared by the authors.

## AUTHOR CONTRIBUTIONS

A.G., J.-J.O.d.X., J.A.M., J.A.P., and J.D. conceived and designed research; A.G., M.E., and S.R.S. performed experiments; A.G., M.E., and S.R.S. analyzed data; A.G., M.E., J.A.P., and J.D. interpreted results of experiments; A.G. prepared figures; A.G. drafted manuscript; A.G., M.E., J.-J.O.d.X., J.A.M., J.A.P., and J.D. edited and revised manuscript; A.G., M.E., J.A.P., and J.D. approved final version of manuscript.

## REFERENCES

- Krakauer JW, Hadjiosif AM, Xu J, Wong AL, Haith AM. Motor learning. *Compr Physiol* 9: 613–663, 2019. doi:10.1002/cphy.c170043.
- Santello M, Baud-Bovy G, Jörntell H. Neural bases of hand synergies. *Front Comput Neurosci* 7: 23, 2013. doi:10.3389/fncom.2013.00023.
- Gentner R, Gorges S, Weise D, Aufm Kampe K, Buttmann M, Classen J. Encoding of motor skill in the corticomuscular system of musicians. *Curr Biol* 20: 1869–1874, 2010. doi:10.1016/j.cub.2010.09.045.
- Kutch JJ, Valero-Cuevas FJ. Muscle redundancy does not imply robustness to muscle dysfunction. *J Biomech* 44: 1264–1270, 2011. doi:10.1016/j.jbiomech.2011.02.014.
- Mollazadeh M, Aggarwal V, Thakor NV, Schieber MH. Principal components of hand kinematics and neurophysiological signals in motor cortex during reach to grasp movements. *J Neurophysiol* 112: 1857–1870, 2014. doi:10.1152/jn.00481.2013.
- Leo A, Handjaras G, Bianchi M, Marino H, Gabicini M, Guidi A, Scilingo EP, Pietrini P, Bicchi A, Santello M, Ricciardi E. A synergy-based hand control is encoded in human motor cortical areas. *eLife* 5: e13420, 2016. doi:10.7554/eLife.13420.
- Hirano M, Funase K. Reorganization of finger covariation patterns represented in the corticospinal system by learning of a novel movement irrelevant to common daily movements. *J Neurophysiol* 122: 2458–2467, 2019. doi:10.1152/jn.00514.2019.
- Waters-Metenier S, Husain M, Wiestler T, Diedrichsen J. Bihemispheric transcranial direct current stimulation enhances effector-independent representations of motor synergy and sequence learning. *J Neurosci* 34: 1037–1050, 2014. doi:10.1523/JNEUROSCI.2282-13.2014.
- Kamara G, Rajchert O, Solomonow-Avnon D, Mawase F. Generalization indicates asymmetric and interactive control networks for multi-finger dexterous movements. *Cell Rep* 42: 112214, 2023. doi:10.1016/j.celrep.2023.112214.
- Fricke C, Gentner R, Alizadeh J, Classen J. Linking individual movements to a skilled repertoire: Fast modulation of motor synergies by repetition of stereotyped movements. *Cereb Cortex* 30: 1185–1198, 2020. doi:10.1093/cercor/bhz159.
- Furuya S, Nakamura A, Nagata N. Acquisition of individuated finger movements through musical practice. *Neuroscience* 275: 444–454, 2014. doi:10.1016/j.neuroscience.2014.06.031.
- Arbuckle SA, Weiler J, Kirk EA, Rice CL, Schieber M, Pruszynski JA, Ejaz N, Diedrichsen J. Structure of population activity in primary motor cortex for single finger flexion and extension. *J Neurosci* 40: 9210–9223, 2020. doi:10.1523/JNEUROSCI.0999-20.2020.
- Park J, Xu D. Multi-finger interaction and synergies in finger flexion and extension force production. *Front Hum Neurosci* 11: 318, 2017. doi:10.3389/fnhum.2017.00318.
- Braido P, Zhang X. Quantitative analysis of finger motion coordination in hand manipulative and gestic acts. *Hum Mov Sci* 22: 661–678, 2004. doi:10.1016/j.humov.2003.10.001.
- Thakur PH, Bastian AJ, Hsiao SS. Multidigit movement synergies of the human hand in an unconstrained haptic exploration task. *J Neurosci* 28: 1271–1281, 2008. doi:10.1523/JNEUROSCI.4512-07.2008.
- Xu J, Mawase F, Schieber MH. Evolution, biomechanics, and neurobiology converge to explain selective finger motor control. *Physiol Rev* 104: 983–1020, 2024. doi:10.1152/physrev.00030.2023.
- Perkins RE, Hast MH. Common variations in muscles and tendons of the human hand. *Clin Anat* 6: 226–231, 1993. doi:10.1002/ca.980060406.
- Zilber S, Oberlin C. Anatomical variations of the extensor tendons to the fingers over the dorsum of the hand: a study of 50 hands and a review of the literature. *Plast Reconstr Surg* 113: 214–221, 2004. doi:10.1097/01.PRS.0000091163.86851.9C.
- Abdel-Hamid GA, El-Beshbishy RA, Abdel Aal IH. Anatomical variations of the hand extensors. *Folia Morphol (Warsz)* 72: 249–257, 2013. doi:10.5603/fm.2013.0040.
- Mosier KM, Scheidt RA, Acosta S, Mussa-Ivaldi FA. Remapping hand movements in a novel geometrical environment. *J Neurophysiol* 94: 4362–4372, 2005. doi:10.1152/jn.00380.2005.

21. **Nazarpour K, Barnard A, Jackson A.** Flexible cortical control of task-specific muscle synergies. *J Neurosci* 32: 12349–12360, 2012. doi:[10.1523/JNEUROSCI.5481-11.2012](https://doi.org/10.1523/JNEUROSCI.5481-11.2012).
22. **Pistohl T, Cipriani C, Jackson A, Nazarpour K.** Abstract and proportional myoelectric control for multi-fingered hand prostheses. *Ann Biomed Eng* 41: 2687–2698, 2013. doi:[10.1007/s10439-013-0876-5](https://doi.org/10.1007/s10439-013-0876-5).
23. **Radhakrishnan SM, Baker SN, Jackson A.** Learning a novel myoelectric-controlled interface task. *J Neurophysiol* 100: 2397–2408, 2008. doi:[10.1152/jn.90614.2008](https://doi.org/10.1152/jn.90614.2008).
24. **Liu X, Scheidt RA.** Contributions of online visual feedback to the learning and generalization of novel finger coordination patterns. *J Neurophysiol* 99: 2546–2557, 2008. doi:[10.1152/jn.01044.2007](https://doi.org/10.1152/jn.01044.2007).
25. **Diedrichsen J, Kornysheva K.** Motor skill learning between selection and execution. *Trends Cogn Sci* 19: 227–233, 2015. doi:[10.1016/j.tics.2015.02.003](https://doi.org/10.1016/j.tics.2015.02.003).
26. **Yokoi A, Diedrichsen J.** Neural organization of hierarchical motor sequence representations in the human neocortex. *Neuron* 103: 1178–1190.e7, 2019. doi:[10.1016/j.neuron.2019.06.017](https://doi.org/10.1016/j.neuron.2019.06.017).
27. **Berlot E, Popp NJ, Diedrichsen J.** A critical re-evaluation of fMRI signatures of motor sequence learning. *eLife* 9: e55241, 2020., doi:[10.7554/eLife.55241](https://doi.org/10.7554/eLife.55241).
28. **Shah NP, Avansino D, Kamdar F, Nicolas C, Kapitonava A, Vargas-Irwin C, Hochberg L, Pandarinath C, Shenoy K, Willett FR, Henderson J.** Pseudo-linear summation explains neural geometry of multi-finger movements in human premotor cortex (Preprint). *bioRxiv*, 2023. doi:[10.1101/2023.10.11.561982](https://doi.org/10.1101/2023.10.11.561982).
29. **Arbuckle SA, Pruszynski JA, Diedrichsen J.** Mapping the integration of sensory information across fingers in human sensorimotor cortex. *J Neurosci* 42: 5173–5185, 2022. doi:[10.1523/JNEUROSCI.2152-21.2022](https://doi.org/10.1523/JNEUROSCI.2152-21.2022).